Paper 7

MASS FLOW PREDICTION IN NATURAL CIRCULATION BOILERS

A. S. T. Thomson* A. W. Scott* D. H. Rooney† A. M. Bradford‡

This paper presents results from a programme of steady-state natural circulation tests carried out on a two-tube experimental boiler. The circuit was constructed using normal commercial tubes and the tests covered the following range of variables:

Tube size:	2¼ in o.d. × 2 s.w.g., 1¾ in o.d. × 4 s.w.g., 1¼ in o.d. × 6 s.w.g.
Tube inclinations:	0, 40, and 60 degrees to vertical
Heat fluxes:	up to 100 000 Btu/h ft^2
Pressures:	200–1000 lbf/in^2 (gauge)
Mass flows obtained:	3×10^5 to 1×10^6 lb/h ft^2
Mass dryness fractions obtained:	0·01–0·36
Void fractions obtained:	0·2–0·9

During the tests, measurements were taken of pressure, pressure difference, circulation rate, and density or void fraction at the top of the riser tube. The void fraction data are presented for use. A theoretical analysis was carried out using an annular type flow model in the riser tube with a simple two-phase friction pressure drop expression which required only void fraction data.

A comparison was made between the theoretical results and the experimental data and the comparison was extended to include (*a*) homogeneous flow, (*b*) Martinelli–Nelson correlation, and (*c*) Thom correlation. The results indicate that the analysis used, which requires only void fraction data, gave the best correlation over the range of natural circulation conditions covered.

INTRODUCTION

THE PRINCIPLES OF NATURAL CIRCULATION in water tube boilers have long been the subject of theoretical study and experiment, and interest in the subject matter, which is basically the thermohydrodynamics of two-phase flow, has been stimulated by the advances made in other fields.

A comprehensive programme of natural circulation tests has been carried out on a high-pressure two-tube experimental boiler located in the University of Strathclyde. This project lasted several years and was initiated and supported by the British Ship Research Association (1)–(5)§, the main application being towards marine boilers although many aspects of the work have a more general application.

The experimental programme and general range of conditions investigated were dictated by the main application, a singular requirement being that normal commercial tubing was used in the circuit. Full details of the range covered are given later.

The method of predicting the mass flow in a natural circulation loop involves satisfying the condition

$$\sum (\text{pressure differences around circuit}) = 0$$

Hence the problem is reduced to one of determining pressure differences under various conditions of single- and two-phase flow. This, in turn, requires information on the slip between the phases (or the void fraction since these are interdependent) and two-phase friction effects. An annular flow type model is proposed for the theoretical predictions of pressure differences in the riser tube and, on this basis, a simple expression for the two-phase friction effects is deduced which requires only void fraction data. Thus, in addition to the usual known information, only void fraction data are required for the pressure difference evaluation, and these have been obtained from experiment.

This paper is confined to a comparison between the experimental circulation, or mass flow rates, and those

The MS. of this paper was received at the Institution on 15th July 1969 and accepted for publication on 18th August 1969. 32

* *Professor, University of Strathclyde, Montrose Street, Glasgow, C.1.*
† *Senior Lecturer. Address as above.*
‡ *Lecturer. Address as above.*

§ *References are given in Appendix 7.3.*

predicted by the theoretical model recommended. The comparison is extended to other theoretical models and correlations including (*a*) homogeneous flow in the riser tube, (*b*) Martinelli–Nelson (**6**) correlation, and (*c*) Thom (7) correlation to illustrate the accuracy, as well as the simplicity, of the recommended analysis.

Notation

c	Circuit constant.
d	Internal diameter of tube.
F	Friction force.
f	Fanning friction factor.
g	Gravitational acceleration.
g_0	Unit system constant.
l	Length.
M	Total mass flow rate.
M_f	Mass flow rate of liquid in two-phase mixture.
M_g	Mass flow rate of steam in two-phase mixture.
p	Pressure.
Δp	Pressure difference.
$\mathrm{d}p/\mathrm{d}l$	Total pressure gradient.
$\mathrm{d}p_F/\mathrm{d}l$	Pressure gradient due to friction.
$\mathrm{d}p_{F_2}/\mathrm{d}p_{F_1}$	Ratio of two-phase friction pressure drop to the corresponding single-phase liquid pressure drop with same total mass flow rate.
s	Slip factor or velocity ratio.
U	Velocity.
U_f	Mean liquid velocity.
U_g	Mean vapour velocity.
v	Specific volume.
v_f	Specific volume of saturated liquid.
v_g	Specific volume of dry saturated vapour.
X	Cross-sectional area of tube.
X_f	Cross-sectional area of tube occupied by liquid.
X_g	Cross-sectional area of tube occupied by vapour.
x_a	Void fraction.
x_m	Mass dryness fraction.
x_v	Volume dryness fraction.
θ	Angle of inclination of tubes to vertical.

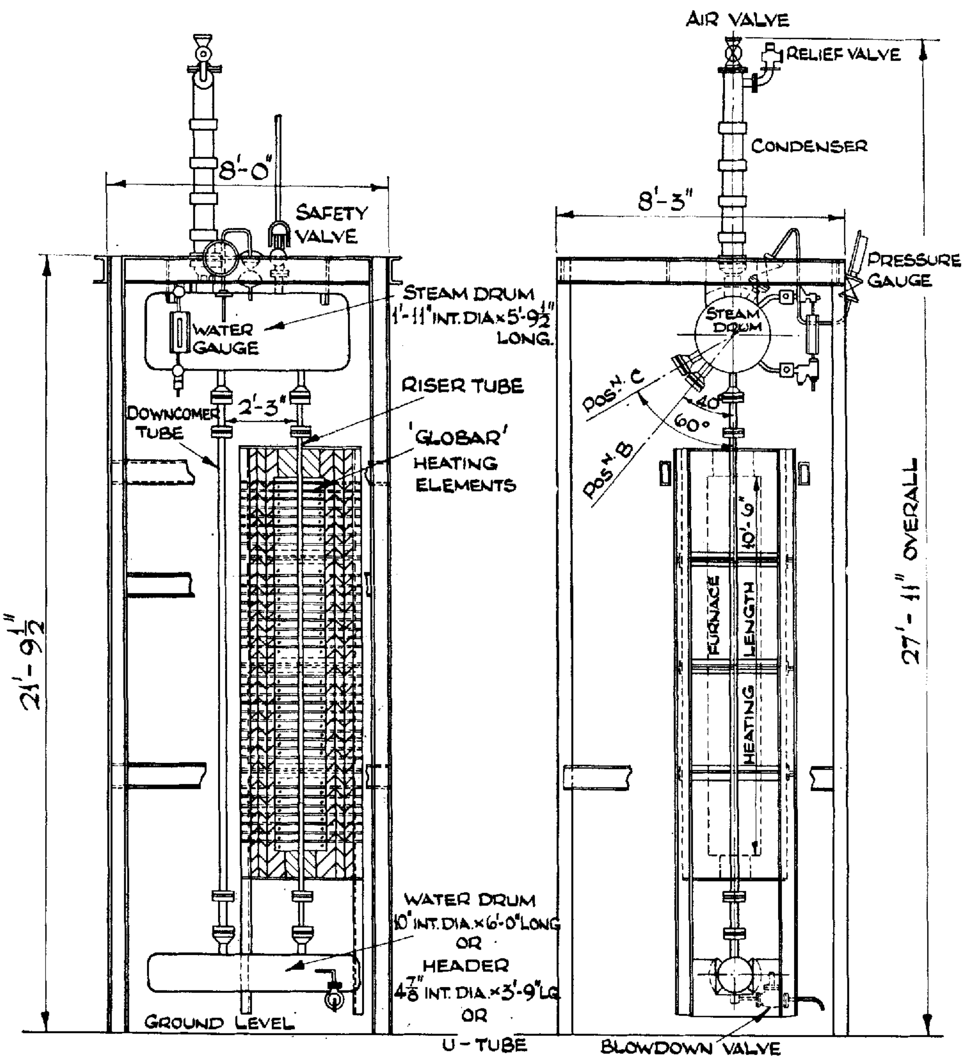

Fig. 7.1. Sketch of experimental boiler and furnace

λ_1 Single-phase friction factor.
λ_2 Two-phase friction factor.
ψ Friction factor ratio.

Subscripts

1 Single-phase flow.
2 Two-phase flow.
a Area.
F Friction.
f Saturated liquid.
g Dry saturated vapour.
M Momentum.
m Mass.
v Volume.

EXPERIMENTAL APPARATUS

The experimental boiler unit used to conduct the circulation tests was a two-tube natural circulation boiler designed for a maximum working pressure of 1500 lbf/in^2 (gauge) with a steam generation of 1200 lb/h when operating with a $2\frac{1}{4}$ in o.d. $\times$ 2 s.w.g. tube, a heated length of 10 ft 6 in, and a heat input rate of 120 000 Btu/h ft^2. The heat input to the riser tube was generated by a 250-kVA electrical furnace and varied by means of a step-change transformer. Provision was made for altering the tube length, diameter, and inclination, and various connections between the bottom ends of the riser and downcomer tubes were used. The arrangement of the boiler and furnace is shown in Fig. 7.1. Details of the dimensions of the circuits used are given in reference (**5**).

In the tests reported here, the plant was operated as a simple closed system in which the steam generated was condensed in a condenser situated on top of the steam drum, the condensate refluxing back into the drum. The pressure in the system was controlled by adjusting the cooling water supply to, and the surface contact area of, this condenser and an energy balance at this point, with due allowance for the apparatus heat losses, gave a measure of the heat input to the riser tube.

Instrumentation

A flow diagram for the closed circuit is shown in Fig. 7.2, which also indicates some of the instrumentation points.

The natural circulation mass flow was obtained by measuring the velocity at the foot of the downcomer tube using a stainless steel pitot tube welded into the tube. The pitot tube was calibrated in situ and connected to a differential pressure pen recorder.

A pressure recorder gave a continuous record of the boiler pressure and was supported by readings from a Bourdon gauge. A differential pressure recorder was connected through manifolds to measure the pressure difference between any two of the following points: steam drum, water drum, riser tube top, riser tube bottom.

Cooling water flow quantities were measured in calibrated tanks and temperatures by mercury thermometers.

The density of the steam–water mixture emerging from the furnace was measured using the gamma-ray technique. This involved passing a collimated beam of gamma rays from a Cs_{137} source through the riser tube where it was attenuated to an extent dependent on the density of the tube contents. The attenuated beam then passed into a cooled ionization chamber where it ionized an inert gas and generated a current between two electrodes. This current was measured as a potential across a very high resistance, suitably amplified and displayed, and hence gave a measure of the density of the tube contents. From the density reading, the void fraction at the sensing point was determined. Fuller details of this method and the results obtained are given in references (**8**)–(**11**); Fig. 7.3 presents void fraction results for use in the analysis.

Other measurements were made during the tests but are not of direct relevance here. A more comprehensive

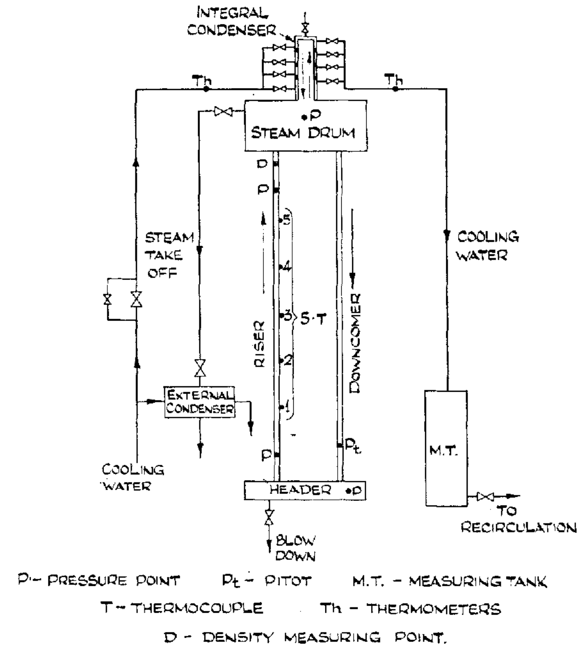

Fig. 7.2. Flow diagram showing instrument points

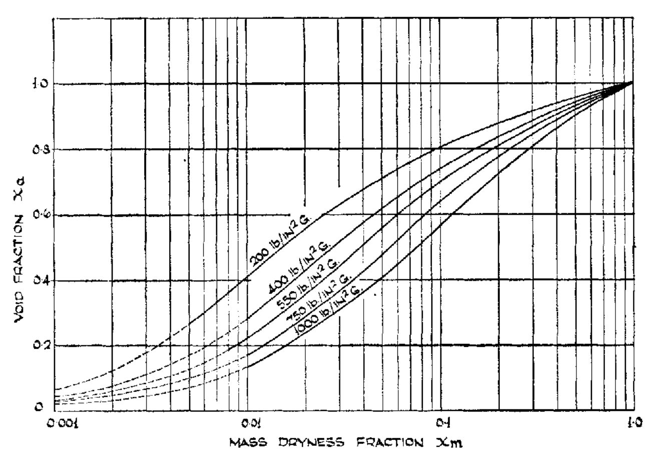

Fig. 7.3. Relationship between void fraction and mass dryness fraction for various pressures

description of the plant and instrumentation is given in references (**9**) and (**12**).

Scope of tests

In any particular series, natural circulation tests were carried out at pressures of 200, 400, 550, 750, and 1000 lbf/in^2 and at five heat inputs ranging from about 20 000 to 100 000 Btu/h ft^2 (based on outside surface area of riser tube).

Test series were completed for three tube sizes ($2\frac{1}{4}$ in o.d. $\times$ 2 s.w.g., $1\frac{3}{4}$ in o.d. $\times$ 4 s.w.g., and $1\frac{1}{4}$ in o.d. $\times$ 6 s.w.g.) with uniform heating over a 10 ft 6 in or 7 ft 6 in effective length. A number of series were duplicated to check the effect of using the header or U-tube connections in place of the water drum. Effects of change in circuit resistance were taken into account in some series by inserting restricting orifices of $\frac{7}{8}$, $\frac{3}{4}$, $\frac{5}{8}$, and $\frac{1}{2}$ in diameter at the bottom of the riser tube. Tests with the tubes inclined at 40 and 60 degrees to the vertical were carried out in addition to vertical tests.

Details of the conditions for the test series considered here are shown in Table 7.1.

THEORETICAL ANALYSIS

In the prediction of mass flows in boilers, the problem reduces to one of balancing the pressure differences in the circuit. For example, the pressure difference between the steam drum and, say, a water drum must be the same whether deduced by way of the downcomer or riser tubes. Deduction of pressure differences in single-phase flow (e.g. downcomer tubes) is relatively simple, whereas that in two-phase flow (e.g. steam–water mixtures in riser tubes) is more complex. Thus the accurate prediction of mass flow, or circulation velocity, is dependent on the ability to deduce accurately the pressure differences in the two-phase flow of steam–water mixtures.

In order to make a theoretical study of the pressure differences in two-phase flow for a particular application, a decision must be made regarding the probable configuration of the two phases comprising the mixture. In this application, an annular type flow model (i.e. annulus of liquid and core of vapour) was adopted to represent the conditions in the riser tube, for the following reasons:

(1) This is, or should be, a desirable region of operation in boilers since the most effective heat transfer performance occurs here.

(2) Such information as is available for the transition to annular flow conditions in the range tested tends to indicate that annular type flow might be expected at mass dryness fractions higher than about 8 per cent in this application.

(3) During the testing on the experimental boiler there was a stability of operation, indicating a stable flow pattern, in almost all of the tests. In a few tests a pulsating type of flow was experienced which caused a sudden decrease in the mass dryness fraction which seemed to indicate the transition from churning or slug type flow to annular flow.

In adopting the annular flow model for conditions in the riser tube it is appreciated that, in the change from single-phase liquid flow, the flow pattern will pass through the bubble flow and slug flow régimes before reaching the annular flow region, and that the length of riser tube occupied by the former régimes will depend on the magnitude of the heat flux. However, it is felt that this is justified in view of the resulting simplicity of the analysis.

In the subsequent analysis of the annular flow model the prediction of the pressure difference components depends on data being available regarding (*a*) void fractions and (*b*) two-phase friction effects. Curves of void fractions, based on Strathclyde data, are presented for use over the range considered, and a simple expression

Table 7.1. Test series identification

Test series number	Tube size: Outside diameter, in	Tube size: Standard wire gauge	Inclination of tube to vertical, θ degrees	Heated length, ft in	Type of circuit	Restricting orifice in riser tube
1	$2\frac{1}{4}$	2	0	10 6	U-tube	None
2	$1\frac{1}{4}$	6	60	10 6	U-tube	None
3	$1\frac{3}{4}$	4	60	10 6	U-tube	None
4	$2\frac{1}{4}$	2	60	10 6	U-tube	None
5	$1\frac{1}{4}$	6	40	10 6	U-tube	None
6	$1\frac{3}{4}$	4	40	10 6	U-tube	None
7	$2\frac{1}{4}$	2	40	10 6	U-tube	None
8	$2\frac{1}{4}$	2	0	10 6	U-tube	None
10	$1\frac{3}{4}$	4	0	7 6	U-tube	None
14	$1\frac{1}{4}$	6	0	10 6	U-tube	None
15	$1\frac{3}{4}$	4	0	10 6	U-tube	None
17	$1\frac{3}{4}$	4	0	10 6	Water drum	None
18	$2\frac{1}{4}$	2	0	10 6	Water drum	$\frac{3}{4}$ in diameter
19	$2\frac{1}{4}$	2	0	10 6	Water drum	None
26	$2\frac{1}{4}$	2	0	10 6	Water drum	$\frac{5}{8}$ in diameter
27	$2\frac{1}{4}$	2	0	10 6	Water drum	$\frac{1}{2}$ in diameter
29	$2\frac{1}{4}$	2	0	10 6	Water drum	$\frac{7}{8}$ in diameter

is also given for friction effects, indicating that the wall friction forces in two-phase flow are similar to those in single-phase liquid flow for the same mean liquid velocity.

Annular flow model

In this model all the liquid is assumed concentrated in an annulus around the tube wall moving with a mean velocity U_{f2} at any section whilst the vapour is concentrated in a central core moving with a mean velocity U_{g2}.

Referring to Fig. 7.4, consider an element of flow of length δl over which the phase velocities change from U_{f2} to $(U_{f2}+\delta U_{f2})$ and from U_{g2} to $(U_{g2}+\delta U_{g2})$ respectively and there is a mass interchange between the phases of δM_g (e.g. evaporation).

If the total cross-sectional area remains constant (as in a normal boiler tube) then a change in the vapour cross-section from X_g to $(X_g+\delta X_g)$ produces a corresponding change in the liquid cross-section from X_f to $(X_f-\delta X_g)$.

Analysing the forces acting on the element, and applying the conservation of momentum, gives

$$pX-(p+\delta p)X-\mathrm{d}F-\frac{g}{g_0}\cos\theta \times\left[\rho_f\left(X_f-\frac{\delta X_g}{2}\right)\delta l+\rho_g\left(X_g+\frac{\delta X_g}{2}\right)\delta l\right] =\frac{1}{g_0}\Big[(M_g+\delta M_g)(U_{g2}+\delta U_{g2}) +(M_f-\delta M_g)(U_{f2}+\delta U_{f2})-M_gU_{g2}-M_fU_{f2}\Big] \quad . \quad . \quad . \quad (7.1)$$

Rearranging, neglecting second-order terms, and substituting the relationships $x_a = X_g/X$ and $(1-x_a) = X_f/X$ gives

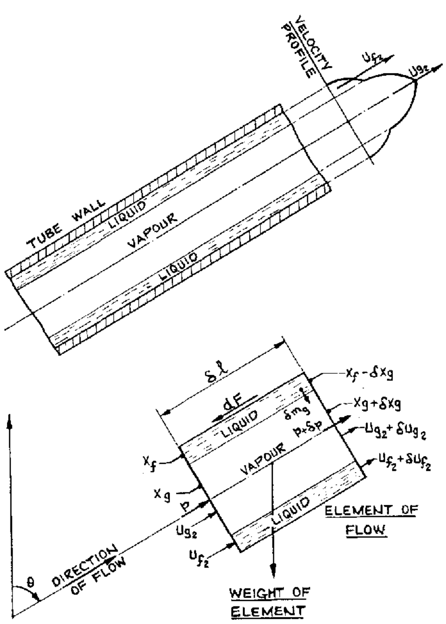

Fig. 7.4. Annular flow model

$$-\frac{\mathrm{d}p}{\mathrm{d}l}=\frac{1}{X}\frac{\mathrm{d}F}{\mathrm{d}l}+\frac{g}{g_0}\cos\theta\left[\frac{1-x_a}{v_f}+\frac{x_a}{v_g}\right] +\frac{1}{g_0X}\frac{\mathrm{d}}{\mathrm{d}l}\left[M_gU_{g2}+M_fU_{f2}\right] \quad (7.2)$$

The three terms on the right-hand side of equation (7.2) are the respective contributions of friction, density, and momentum effects.

Thus, in order to deduce two-phase pressure differences, information is required regarding (*a*) void fractions, which give a measure of the slip between the phases, (*b*) two-phase friction effects, and (*c*) momentum effects. These are now dealt with in turn. Some useful relationships obtained by applying the conservation of mass are shown in Appendix 7.1.

Void fractions

As previously stated, the method of measuring void fractions by the gamma-ray technique, together with the results obtained and a comparison with the data from other sources, has been reported previously (8)–(11) and the Strathclyde data shown in Fig. 7.3 are presented for use here. The data are plotted as void fraction against mass dryness fraction for the various pressures considered with no appreciable mass velocity effects over the range of natural circulation conditions considered.

Two-phase friction effects

In general, for a fluid flowing in a turbulent condition past a solid boundary, the drag force F exerted by the fluid can be expressed in terms of a friction coefficient, a characteristic area, and the mean kinetic energy per unit volume of the fluid. The pressure gradient due to this drag force, for a circular tube, becomes

$$\frac{\mathrm{d}p_F}{\mathrm{d}l}=\frac{\lambda U^2}{2g_0\,\mathrm{d}v} \quad . \quad . \quad . \quad (7.3)$$

where $\lambda = 4f =$ friction factor.

For single-phase liquid flow, equation (7.3) becomes

$$\frac{\mathrm{d}p_{F1}}{\mathrm{d}l}=\frac{\lambda_1 U_{f1}^{\,2}}{2g_0\,\mathrm{d}v_f} \quad . \quad . \quad . \quad (7.4)$$

The velocity profile under such conditions is shown by $0abcb'a'0'$ in Fig. 7.5.

Consider now this single-phase flow to be artificially divided into an annulus and a core of the fluid, the velocity profiles being exactly similar to the single-phase condition. Let the mean velocity in the annulus of fluid be U'_{f2} then the pressure gradient due to friction will be similar to equation (7.4) and can be expressed, by considering the annulus only, as

$$\frac{\mathrm{d}p'_{F2}}{\mathrm{d}l}=\frac{\lambda_1(U'_{f2})^2c_1^{\,2}}{2g_0\,\mathrm{d}v_f} \quad . \quad . \quad (7.5)$$

where $c_1 = U_{f1}/U'_{f2}$.

Equation (7.5) would also hold for the two-phase case provided the velocity profile was the same as for the single-phase case.

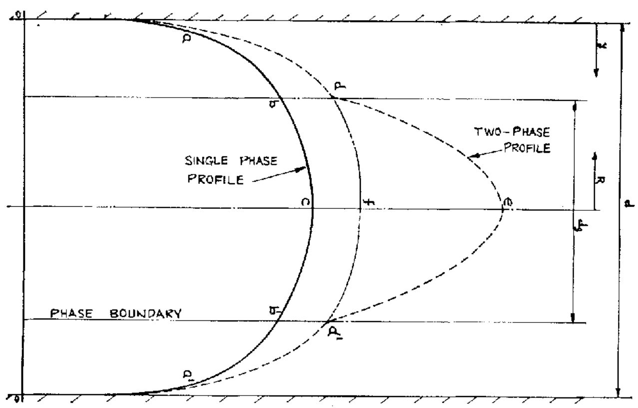

Fig. 7.5. Velocity profiles in single- and two-phase flow

In fact, under two-phase annular flow conditions, the velocity profile of the liquid annulus will be distorted due to the drag exerted on it by the faster moving gas core and will take a form similar to the dotted curve shown in Fig. 7.5.

If the mean velocity in the liquid annulus under these actual two-phase flow conditions is U_{f_2}, then the pressure gradient due to friction may be written as

$$\frac{\mathrm{d}p_{F2}}{\mathrm{d}l}=\frac{\lambda_1 U_{f_2}{}^2 c_2{}^2\phi}{2g_0\,\mathrm{d}v_f} \quad . \quad . \quad (7.6)$$

where $c_2 = U'_{f_1}/U_{f_2}$, U'_{f_1} is the mean velocity for single-phase flow across the tube cross-section with a velocity profile matching that in the annulus (i.e. curve $0dfd'0'$ in Fig. 7.5) and ϕ is a factor introduced to allow for any profile distortion effects not covered by c_2, e.g. change in λ_1 due to change in Reynolds number.

Equation (7.6) may then be written as

$$\frac{\mathrm{d}p_{F2}}{\mathrm{d}l}=\frac{\psi\lambda_1 U_{f_2}{}^2}{2g_0\,\mathrm{d}v_f} \quad . \quad . \quad . \quad (7.7)$$

where $\psi = c_2{}^2\phi = \lambda_2/\lambda_1$ (λ_2 = two-phase friction factor). This gives an expression for the two-phase friction pressure gradient analogous to that for single-phase flow in equation (7.4). Substituting for U_{f_2} from equations (7.15) and (7.13) in Appendix 7.1 gives

$$\frac{\mathrm{d}p_{F2}}{\mathrm{d}l}=\frac{\psi\lambda_1 U_{f_1}{}^2}{2g_0\,\mathrm{d}v_f}\cdot\frac{(1-x_m)^2}{(1-x_a)^2} \quad . \quad . \quad (7.8)$$

which requires, in addition to the void fraction data already presented, values of the friction factor ratio ψ.

Friction factor ratio ψ

In order to obtain information on the friction factor ratio ψ, a review of the literature on two-phase friction effects was undertaken. The results from many publications were analysed with no great success due to the variety of conditions involved. Details of this are given in references (**5**) and (**9**).

In the analysis reported here, a value of $\psi = 1$ was used and this provided a simple and convenient method of determining the two-phase friction effects. Justification for the use of $\psi = 1$ is presented, both theoretically and experimentally, in Appendix 7.2.

Putting $\psi = 1$ simplifies equation (7.8) to

$$\frac{\mathrm{d}p_{F2}}{\mathrm{d}l}=\frac{\lambda_1 U_{f_1}{}^2}{2g_0\,\mathrm{d}v_f}\cdot\frac{(1-x_m)^2}{(1-x_a)^2} \quad . \quad . \quad (7.9)$$

and allows the two-phase friction pressure gradient to be found using the void fraction data given in Fig. 7.3.

Expressions similar to equation (7.9) have been proposed elsewhere, e.g. references (**13**) (**14**), and an attempt has been made here to justify the use of such an expression and, at the same time, provide the necessary void fraction data required in the evaluation.

Two-phase momentum effects

The pressure gradient due to momentum changes under annular flow conditions was given earlier as the last term in equation (7.2). Substituting the relationships in Appendix 7.1 where necessary, this becomes

$$\frac{\mathrm{d}p_M}{\mathrm{d}l}=\frac{M^2}{X^2 g_0}\cdot\frac{\mathrm{d}x_m}{\mathrm{d}l}\left[2\left\{\frac{x_m}{x_a}v_g-\frac{1-x_m}{1-x_a}v_f\right\}-\frac{\mathrm{d}x_a}{\mathrm{d}x_m}\left\{\frac{x_m{}^2}{x_a{}^2}v_g-\frac{(1-x_m)^2}{(1-x_a)^2}v_f\right\}\right] \quad (7.10)$$

In the case of uniform heating, the mass dryness fraction may be assumed to vary linearly with length making $\mathrm{d}x_m/\mathrm{d}l$ constant.

Application to experimental boiler

In the prediction of mass flows, the basic criterion to be satisfied is

$$\sum(\text{pressure differences around circuit}) = 0 \quad (7.11)$$

Energy balances allow us to find the mass dryness fraction leaving the furnace and the point in the riser tube where evaporation starts. This, in turn, defines the parts of the circuit which involve single-phase flow, two-phase evaporative flow, and two-phase adiabatic flow.

In the single-phase part of the circuit the total pressure difference is composed of density and friction components together with losses due to bends, entry, and restrictions. The last group can be expressed in the form $c(U_{f_1}{}^2/v_f)$, where c is a constant for a particular circuit.

In the two-phase evaporative length, which extends from the point of start of evaporation to the furnace top, the mass dryness fraction varies linearly with length under uniform heating conditions. Values of the pressure gradient at a number of sections in this length were deduced from equations (7.2), (7.9), and (7.10) and summed to give the total pressure difference over this length.

In the two-phase adiabatic length the mass dryness fraction remains effectively constant with momentum effects zero. Thus, only density and friction need be considered in deducing the pressure difference.

The method of predicting the mass flow in the circuit involved an iterative procedure of assuming a mass flow rate and then deducing the pressure distribution around the circuit until equation (7.11) was satisfied.

CIRCULATION RESULTS

A total of 17 test series were analysed comprising 385 different test conditions over the range indicated in Table 7.1. Each test series generally comprised five heat input rates at the standard pressures of 200, 400, 550, 750, and 1000 lbf/in^2 (gauge).

The experimental values of circulation velocity or mass flow rate were compared with values predicted using the theory previously outlined and a percentage error deduced, relative to the experimental value. In addition, comparative theoretical values of mass flow rate were deduced using the homogeneous flow model and the correlations proposed by Martinelli–Nelson (**6**) and Thom (**7**).

Full details of the results obtained are given in reference (**9**) with a summary presented in Tables 7.2 and 7.3. Table 7.2 gives a comparison between the four theories used in the analysis as regards accuracy of prediction, by showing the number of tests falling within a particular error range. Each range is further subdivided into high and low values.

A further comparison is made in Table 7.3 where, in addition to the overall accuracy being quoted, the effects of tube flow pressure, mass dryness fraction, and mass flow rate on accuracy are examined.

General information on the range of variables covered is given in Table 7.4.

DISCUSSION OF RESULTS

The most striking feature about the data shown in Tables 7.2 and 7.3 is the close agreement between the results obtained using the proposed theory and the improvement in mass flow prediction obtained by this theory over the others, in particular with respect to the homogeneous flow theory. The overall arithmetic mean differences between the experimental value of mass flow and those predicted by the proposed theory, the homogeneous flow theory, the Martinelli–Nelson model, and the Thom model are, respectively, 6·5, 14·5, 7·3, and 9·6 per cent.

Tables 7.2 and 7.3 give other statistics of the correlation and indicate that for the 385 test conditions analysed the proposed theory successfully predicted the mass flow to within ± 10 per cent in 83 per cent of the conditions. This is considerably better than the homogeneous flow theory figure of 47 per cent and the Thom annular flow model with 59 per cent and is also an improvement on the Martinelli–Nelson model which predicted 76 per cent of the tests covered to within ± 10 per cent.

Further evidence of the success of the proposed theory is given in Table 7.2, which indicates that only in 6 per cent of the test conditions covered was the percentage deviation of the predicted mass flow from the experimental greater than ± 15 per cent.

Another notable feature from Table 7.2 is that the proposed theory, in contrast to other theories, predicts a mass

Table 7.2. Number of tests falling within a particular error range (expressed as percentage)

Error range, per cent	Proposed model, per cent		Homogeneous model, per cent		Martinelli–Nelson model, per cent		Thom model, per cent	
	High	Low	High	Low	High	Low	High	Low
0 to 10	28	55	39·2	7·8	40·5	35·3	22·9	35·8
10 to 15	3·7	7	14	0·3	8·5	5·5	10·2	11·8
15 to 20	1·6	2·3	9·6	0	2·9	1	4·7	3·6
20 to 25	0·5	1·3	12·5	0	2·9	1	5·2	1·6
25 to 30	0·25	0·25	5·4	0	1·6	0	2·6	0
Above 30	0	0	11·2	0	0·8	0	1·6	0

Table 7.3. Arithmetic mean errors for various ranges

Test range	Proposed model, per cent	Homogeneous model, per cent	Martinelli–Nelson model, per cent	Thom model, per cent	Number of tests
Overall	6·5	14·5	7·3	9·6	385
$1\frac{1}{4}$-in tube	10·2	26·3	11·2	16·8	71
$1\frac{3}{4}$-in tube	5·2	18·6	7·1	8·7	125
$2\frac{1}{4}$-in tube	6·5	7·9	6·3	7·8	189
Pressure: 200 lbf/in^2 (gauge)	6·9	13·7	7·0	10·5	79
400 lbf/in^2 (gauge)	6·1	14·9	7·2	9·6	83
550 lbf/in^2 (gauge)	6·4	14·5	7·7	9·5	83
750 lbf/in^2 (gauge)	6·6	15·3	7·9	9·3	70
1000 lbf/in^2 (gauge)	6·9	13·7	6·6	8·4	70
$x_m < 0·05$	6·5	11·7	8·3	8·5	173
$0·05 \leqslant x_m < 0·1$	6·2	13·4	6·1	7·4	127
$x_m \geqslant 0·1$	7·5	21·8	6·9	14·6	85
$M/X \geqslant 5 \times 10^5$ lb/h ft^2	5·7	10·8	6·0	7·4	257
$M/X < 5 \times 10^5$ lb/h ft^2	8·3	21·8	9·8	14·1	128

Table 7.4. General information on range of variables covered

Variable	*Range*
Solid-drawn mild steel commercial tubes	$1\frac{1}{4}$ in o.d. × 6 s.w.g. $1\frac{3}{4}$ in o.d. × 4 s.w.g. $2\frac{1}{4}$ in o.d. × 2 s.w.g.
Tube inclination to vertical	0, 40 and 60 degrees
Single-phase friction factors for tubes tested	
$1\frac{1}{4}$-in o.d. tube	0·0325
$1\frac{3}{4}$-o.d. tube	0·032
$2\frac{1}{4}$-in o.d. tube	0·0292
$2\frac{1}{4}$-in o.d. tube with $\frac{7}{8}$-in orifice	0·022
$2\frac{1}{4}$-in o.d. tube with $\frac{3}{4}$-in orifice	0·026
$2\frac{1}{4}$-in o.d. tube with $\frac{5}{8}$-in orifice	0·024
$2\frac{1}{4}$-in o.d. tube with $\frac{1}{2}$-in orifice	0·024
Heat input, Btu/h ft² (external)	100 000
Pressure, lbf/in² (gauge)	200 to 1000
Mass flow rates, lb/h ft²	3×10^5 to 1×10^6
Mass dryness fraction	0·01 to 0·36
Void fraction	0·2 to 0·9
Volumetric dryness fraction	0·26 to 0·971
Circulation velocity, ft/s	1·5 to 4·95
Mean steam velocity, ft/s	4·5 to 66
Mean water velocity, ft/s	3·14 to 16·4
Non-slip mixture velocity, ft/s	3·50 to 60·1

flow value which is on the low side in two cases out of three. Certain comfort is gained from this in so far as the lower-than-experimental mass flow values will yield higher-than-experimental mass dryness fraction values at the rise tube top thereby promoting safety.

The statistics of Table 7.3 were compiled in an attempt to study the individual effects of tube size, quality, pressure, and mass flow on the accuracy of prediction. It is noticeable that the mean errors are much higher for the smallest size of tube, this being consistent for all four theories. This may be due to the annular flow pattern being close to breakdown in the smallest (0·866 i.d.) tubes, as is evidenced by the fact that in a few cases the flow did break down into a pulsating type flow at the lower pressures.

There is no noticeable effect of pressure on the accuracy of prediction, it being almost uniform over the pressure range from 200 to 1000 lbf/in². This is verified from the results for the other theories.

The effect of mass dryness fraction on accuracy is not noticeable for the proposed theory, at least over the range covered. It is to be expected that the annular flow pattern will be strengthened at the higher qualities, and this is borne out by the fact that for the homogeneous flow theory the accuracy of prediction falls off at the higher qualities.

Comparative figures for accuracy have also been deduced for mass flow rates above and below 5×10^5 lb/h ft³ and although there is little effect on the proposed theory and the Martinelli–Nelson model, the homogeneous flow model shows a marked improvement at the higher flow rates. This may be attributed to greater turbulence and more disturbance of the flow pattern at these higher flow rates, so favouring homogeneity.

The expression proposed for evaluating the two-phase friction effects is fairly simple, with $\psi = 1$, and required only void fraction data for the solution. With $\psi = 1$ this means the two-phase friction factor equals the single-phase friction factor when it is based on the mean liquid velocity and density in the annulus. This gives

$$\frac{dp_{F_2}}{dp_{F_1}} = \frac{(1-x_m)^2}{(1-x_a)^2}$$

and indicates that, at least for vertical upflow, two-phase friction effects will exceed single-phase effects.

It is recognized that equation (7.9), with $\psi = 1$, is probably an oversimplification as regards a general solution to two-phase effects although, when applied to the natural circulation range covered here, it yielded good results. It may be that over a wider range the mass flow will have an effect on ψ and in a circuit with horizontal two-phase lengths, where friction effects are not swamped by the density pressure drop effects, further refinement is necessary. However, the use of equation (7.9) has the merit that it forges the two 'missing links' of information (i.e. void fractions and two-phase friction) into one since the friction effects are expressed in terms of void fraction and other known quantities.

A fairly extensive programme of experimental work over a wide range of mass flows, concentrating on two-phase friction effects amongst other things, is at present being conducted at the University of Strathclyde with a modified apparatus.

CONCLUSIONS

The proposed model successfully predicts the natural circulation velocity or mass flow, over the range investigated, to within ±10 per cent in 83 per cent of the test conditions covered. In only 6 per cent of the tests did the error exceed ±15 per cent. This is better than the other models used in the comparison, and considerably better than the homogeneous flow theory.

Information regarding void fraction, or slip effects between the steam and water, is adequately supplied in Fig. 7.3. It was found that, over the range tested, the effects of mass flow were so small as to be negligible.

The complexities of two-phase friction effects have been reduced to a simple expression involving void fraction, a two-phase friction factor, and other known quantities. It is further simplified since the results from theory and other workers suggest that, over the range tested, the two-phase friction factor equals the single-phase friction factor when applied to the mean liquid velocity and liquid density in the two-phase mixture.

ACKNOWLEDGEMENTS

This project was supported financially by the British Ship Research Association and the authors gratefully acknowledge this and the help received from the Association staff at all times.

APPENDIX 7.1

RELATIONSHIPS IN TWO-PHASE ANNULAR FLOW

Total cross-section area is

$$X = X_f + X_g \quad . \quad . \quad . \quad (7.12)$$

Total mass flow is

$$\begin{aligned} M &= M_f + M_g \\ &= (1-x_m)M + x_m M \\ &= \frac{U_{f2}X_f}{v_f} + \frac{U_{g2}X_g}{v_g} \\ &= \frac{U_{f1}X}{v_f} \quad . \quad . \quad . \quad . \quad . \quad (7.13) \end{aligned}$$

Mean vapour velocity is

$$U_{g2} = \frac{x_m M v_g}{X_g} = \frac{x_m}{x_a} \cdot \frac{M}{X} v_g \quad . \quad (7.14)$$

Mean liquid velocity is

$$U_{f2} = \frac{(1-x_m)Mv_f}{X_f} = \frac{(1-x_m)}{(1-x_a)} \cdot \frac{M}{X} v_f \quad (7.15)$$

Slip factor is

$$s = \frac{U_{g2}}{U_{f2}} = \frac{x_m}{(1-x_m)} \cdot \frac{(1-x_a)}{x_a} \cdot \frac{v_g}{v_f} \quad . \quad (7.16)$$

From equation (7.15), the void fraction is

$$x_a = \frac{x_m v_g}{x_m v_g + s(1-x_m)v_f} \quad . \quad . \quad (7.17)$$

From equations (7.15) and (7.17)

$$U_{g2} = \frac{M}{X}[x_m v_g + s(1-x_m)v_f] \quad . \quad (7.18)$$

and

$$U_{f2} = \frac{M}{X}\left[\frac{x_m v_g}{s} + (1-x_m)v_f\right] \quad . \quad (7.19)$$

The volume dryness fraction is

$$x_v = \frac{x_m v_g}{x_m v_g + (1-x_m)v_f} \quad . \quad . \quad (7.20)$$

which is equal to x_a where no slip takes place.

APPENDIX 7.2

FRICTION FACTOR RATIOS

As indicated under 'Friction factor ratio ψ', the value of ψ used in the analysis was unity. The theoretical and experimental justifications for using such a value are given below.

Theoretical

Referring to the velocity profiles shown in Fig. 7.5, and to equation (7.6) which yields

$$\frac{dp_{F2}}{dl} = \frac{\lambda'_1 U'^2_{f1}}{2g_0 \, dv_f}$$

where λ'_1 and U'_{f1} refer to profile $0dfd'0'$, U'_{f1} being the mean velocity over the tube cross-section from this profile,

$$\frac{dp_{F2}}{dp_{F1}} = \frac{\lambda'_1}{\lambda_1} \cdot \frac{U'^2_{f1}}{U^2_{f1}} \quad . \quad . \quad (7.21)$$

Expressing λ in the general form $\lambda = c(Re)^n$, then

$$\frac{dp_{F2}}{dp_{F1}} = \left[\frac{U'_{f1}}{U_{f1}}\right]^{2+n} \quad . \quad . \quad (7.22)$$

Assuming the annulus to be in turbulent flow and obeying the 'one-seventh' law, the velocity at radius R on profile $0dfd'0'$ can be expressed by

$$U = U_{\max}\left(1 - \frac{2R}{d}\right)^{1/7} \quad . \quad . \quad (7.23)$$

where d is the tube diameter. Thus

$$U'_{f1} = \frac{4}{\pi d^2}\int_0^{d/2} U_{\max}\left(1-\frac{2R}{d}\right)^{1/7} 2\pi R \, dR$$

Let $y = d/2 - R$, then $dy/dR = -1$. Therefore

$$U'_{f1} = \frac{8U_{\max}}{d^2}\int_0^{d/2}\left(\frac{2y}{d}\right)^{1/7}\left(\frac{d}{2}-y\right) dy$$

which reduces to

$$U'_{f1} = \frac{49}{60} U_{\max} \quad . \quad . \quad (7.24)$$

The mean liquid velocity in the annulus, U_{f2}, is given by

$$U_{f2} = \frac{4}{\pi(d^2 - d_g^2)}\int_{d_g/2}^{d/2} U_{\max}\left(1-\frac{2R}{d}\right)^{1/7} 2\pi R \, dR$$

where d_g is the diameter of vapour core.

Hence, using a similar substitution,

$$U_{f2} = \frac{2U_{\max}}{(d^2 - d_g^2)d^{1/7}}\left[\frac{7}{8}d(d-d_g)^{8/7} - \frac{7}{15}(d-d_g)^{15/7}\right]$$

but $$x_a = \frac{X_g}{X} = \frac{d^2_g}{d^2}$$

therefore $$d_g = \sqrt{x_a} . d$$

Thus

$$U_{f2} = \frac{2U_{\max}}{(1-x_a)}\left[\frac{7}{8}(1-\sqrt{x_a})^{8/7} - \frac{7}{15}(1-\sqrt{x_a})^{15/7}\right] \quad . \quad . \quad . \quad (7.25)$$

But from equation (7.15)

$$U_{f2} = \frac{1-x_m}{1-x_a} \cdot \frac{M}{X} v_f$$

therefore,

$$U_{\max} = \frac{1-x_m}{2} \cdot \frac{M}{X} v_f \left[\frac{7}{8}(1-\sqrt{x_a})^{8/7} - \frac{7}{15}(1-\sqrt{x_a})^{15/7}\right] \quad . \quad . \quad . \quad (7.26)$$

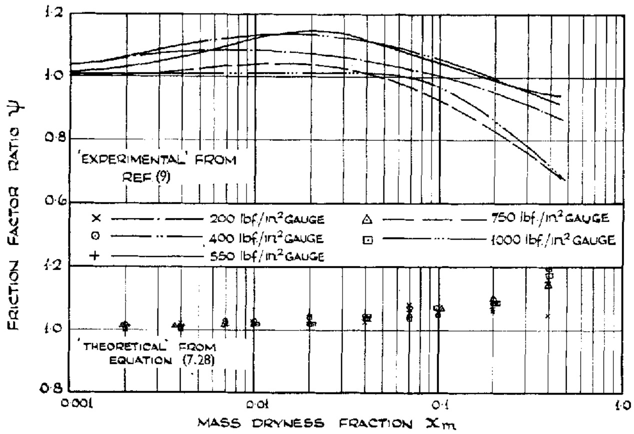

Fig. 7.6. Friction factor ratios

and substituting equations (7.13), (7.24), and (7.26) into equation (7.24) gives

$$\frac{\mathrm{d}p_{F_2}}{\mathrm{d}p_{F_1}} = \frac{49}{120}(1-x_m) \times \left[\frac{7}{8}(1-\sqrt{x_a})^{8/7} - \frac{7}{15}(1-\sqrt{x_a})^{15/7}\right]^{-2-n}$$

For turbulent flow in tubes $n \doteqdot -0{\cdot}25$, decreasing to zero with very rough tubes. Considering $n = -0{\cdot}25$, then

$$\frac{\mathrm{d}p_{F_2}}{\mathrm{d}p_F} = \left[\frac{7(1-x_m)}{15(1-\sqrt{x_a})^{8/7} - 8(1-\sqrt{x_a})^{15/7}}\right]^{1{\cdot}75} \quad (7.27)$$

Combining equations (7.4) and (7.7) gives

$$\psi = \frac{(1-x_a)^2}{(1-x_m)^2} \cdot \frac{\mathrm{d}p_{F_2}}{\mathrm{d}p_{F_1}}$$

hence

$$\psi = \frac{(1-x_a)^2}{(1-x_m)^2}\left[\frac{7(1-x_m)}{15(1-\sqrt{x_a})^{8/7} - 8(1-\sqrt{x_a})^{15/7}}\right]^{1{\cdot}75} \quad . \quad . \quad . \quad (7.28)$$

Using the void fraction data presented in Fig. 7.3, values of ψ were deduced from equation (7.28) for the range of pressures being investigated, and these are shown in Fig. 7.6.

Experimental

For experimental backing, the friction factor data of Haywood (**15**) was chosen because it was obtained from a water tube boiler operating under the same range of conditions, approximately. The friction factor data presented were based on the mean bulk velocity of the steam–water mixture, and this had to be converted to the mean liquid velocity basis of equation (7.7). The transformation took the form

$$\psi = \frac{(1-x_a)^2}{(1-x_m)^2}\left[\frac{x_m v_g + (1-x_a)v_f}{v_f}\right]\frac{\lambda'_2}{\lambda_1}$$

where λ_1 was the friction factor based on the mean bulk velocity, and the void fraction data of Fig. 7.3 were used to produce the typical curve of ψ against x_m shown in Fig. 7.6.

The curves shown in Fig. 7.6, both theoretical and experimental, indicate that over a wide range of x_m values the approximation of $\psi = 1$ was justified.

APPENDIX 7.3

REFERENCES

(**1**) THOMSON, A. S. T., SCOTT, A. W., LAIRD, A. M. and CHISHOLM, D. 'First report: The effect on natural circulation of uniform and non-uniform heat input at steam pressures up to 1500 lbf/in² with vertical tubes', *B.S.R.A. Rept No. 124* 1954.

(**2**) THOMSON, A. S. T., SCOTT, A. W. and LAIRD, A. M. 'Second report: Further tests on the effect of natural circulation of heat input at steam pressures up to 1500 lbf/in²', *B.S.R.A. Rept No. 180* 1955.

(**3**) THOMSON, A. S. T., SCOTT, A. W. and LAIRD, A. M. 'Third report: Measurement of density of steam–water mixtures in boiler tubes by gamma-ray technique', *B.S.R.A. Rept No. 330* 1961.

(**4**) THOMSON, A. S. T., SCOTT, A. W., LAIRD, A. M., ROONEY, D. H. and BRADFORD, A. M. 'Fourth report: Further results from natural circulation tests including inclined tube tests', *B.S.R.A. Rept NS 5* 1963.

(**5**) THOMSON, A. S. T., SCOTT, A. W., LAIRD, A. M., ROONEY, D. H. and BRADFORD, A. M. 'Final report: Circulation velocity prediction in boiler design', *B.S.R.A. Rept NS 50* 1964.

(**6**) MARTINELLI, R. C. and NELSON, D. B. 'Prediction of pressure drop during forced circulation of boiling water', *Trans. Am. Soc. mech Engrs* 1948 **70** (No. 6).

(**7**) THOM, J. R. S. 'Prediction of pressure drop during forced circulation boiling of water', *Int. J. Ht Mass Transfer* 1964 **7** (No. 7).

(**8**) ROONEY, D. H. 'The measurement of void fraction or density using gamma rays', *N.E.L. Rept No. 217* 1966.

(**9**) ROONEY, D. H. 'Natural circulation velocity prediction with particular reference to water tube boilers', Ph.D. thesis, University of Strathclyde, 1967.

(**10**) LAIRD, A. M., SCOTT, A. W. and THOMSON, A. S. T. 'Two-phase flow in the riser tube of an experimental two-tube boiler', *Symp. Two-Phase Fluid Flow*, London 1962 (February) (Instn Mech. Engrs, London).

(**11**) SIMPSON, H. C. and ROONEY, D. H. 'Void fraction prediction under saturation conditions', *N.E.L. Rept No. 386* 1969.

(**12**) LAIRD, A. M., SCOTT, A. W. and THOMSON, A. S. T. 'Natural circulation investigations on an experimental two-tube boiler', *Trans. NE Cst Instn Engrs Shipbldrs* 1958 **74**, 311.

(**13**) LINNING, D. L. 'The adiabatic flow of evaporating fluids in pipes of uniform bore', *Proc. Instn mech. Engrs* 1952 **1B** (No. 2).

(**14**) LINNING, D. L., PEXTON, A. F. and ALDERSON, M. A. H. G. 'Evaporating fluid flow in pipes: A theory for the prediction of phase velocity, pressure drop and critical outlet conditions for evaporating annular flow in pipes', *J. mech. Engng Sci.* 1968 **10**, 64.

(**15**) HAYWOOD, R. W., KNIGHTS, G. A., MIDDLETON, G. E. and THOM, J. R. S. 'Experimental study of the flow conditions and pressure drop of steam–water mixtures at high pressures in heated and unheated channels', *Proc. Instn mech. Engrs* 1961 **175** (13), 669.